THE JOURNAL OF BIOLOGICAL CHEMISTRY VOL. 283, NO. 43, pp. 28918–28925, October 24, 2008

Phorbol Ester-dependent Phosphorylation Regulates the Association of p57/Coronin-1 with the Actin Cytoskeleton*

Received for publication, December 7, 2007, and in revised form, July 16, 2008 Published, JBC Papers in Press, August 7, 2008, DOI 10.1074/jbc.M709990200

Teruaki Oku[‡], Yutaka Kaneko[‡], Koki Murofushi[‡], Yoshiyuki Seyama[§], Satoshi Toyoshima[¶], and Tsutomu Tsuji[‡1]

From the [‡]Department of Microbiology and the [§]Department of Clinical Chemistry, Hoshi University School of Pharmacy and Pharmaceutical Sciences, Tokyo 142-8501, Japan and the [¶]Pharmaceuticals and Medical Devices Agency, Tokyo 100-0013, Japan

The p57/coronin-1 protein is a member of the coronin family of actin-binding proteins, which are characterized by the presence of WD (tryptophan/aspartic acid) repeats and a coiled-coil motif in the molecule. It is selectively expressed in immune cells and has been suggested to play crucial roles in leukocyte functions, including cell migration and phagocytosis. In this study we examined the effects of p57/coronin-1 phosphorylation on the association of the protein with actin. Treatment of HL60 human leukemic cells or p57/coronin-1-transfected HEK293 cells with phorbol 12-myristate 13-acetate (PMA) reduced the association of p57/coronin-1 with the actin cytoskeleton, as indicated by cell fractionation experiments and by fluorescence microscopic observation. Two-dimensional gel electrophoresis of HL60 cell lysate revealed that p57/coronin-1 was phosphorylated upon PMA stimulation of the cells, giving two major and two minor spots of phosphorylated forms, each with distinct isoelectric points. The p57/coronin-1 molecules associated with the cytoskeleton in PMA-treated HL60 cells were phosphorylated at lower levels than those recovered in the cytosolic fraction. In addition, p57/coronin-1 co-sedimented with F-actin polymerized *in vitro* had lower phosphorylation levels than the molecules remaining in the supernatant. By affinity chromatographic analysis using anti-p57/coronin-1 antibody-conjugated Sepharose, p57/coronin-1 derived from PMA-treated HL60 cells showed lower affinity for actin than that from untreated cells. Finally, recovery of p57/coronin-1 in the actin cytoskeleton-rich fraction from neutrophil-like differentiated HL60 cells decreased during phagocytosis, concomitant with enhanced phosphorylation of p57/coronin-1. These results strongly suggest that the phosphorylation of p57/coronin-1 down-regulates its association with actin and modulates the reorganization of actin-containing cytoskeleton.

Actin-binding proteins participate in a variety of leukocyte functions, including chemotaxis, phagocytosis, degranulation, and cellular signaling via reorganization of the actin cytoskeleton. Coronin is an actin-binding protein originally found in *Dictyostelium discoideum* (1) and has been reported to play important roles in migration, phagocytosis, and cell division of myxomycetes (2–7). Many homologous proteins to coronin were successively identified in various eukaryotes from yeasts to mammals (8). In humans, seven homologues have been identified, and collectively they constitute the coronin protein family. This family is characterized by common structural features, such as five WD (tryptophan-aspartic acid) repeats located at the center of the molecule and a coiled-coil domain at the C terminus. Each coronin member exhibits distinct tissue distribution, suggesting each has a specific function in various actin-related cellular processes in respective tissues (9). We previously identified p57/coronin-1 as the first mammalian coronin and found its selective expression in immune cells (10). We have also reported that p57/coronin-1 possesses at least two actin binding sites in the N-terminal region (11) and forms a dimeric structure via the leucine zipper motif in the C-terminal coiled-coil region (12). These results suggest that p57/coronin-1 is involved in the regulation of the rearrangement of the actin-containing cytoskeleton through the cross-linking and bundling of filaments. Recent reports by Yan *et al.* (13, 14) indicated that p57/coronin-1 was actively involved in chemotaxis and phagosome formation in leukocytes. p57/coronin-1 accumulated at the leading edge of migrating neutrophils and in the nascent phagosome, and the introduction of a dominant-negative form or TAT fusion construct of p57/coronin-1 into leukocytes resulted in the inhibition of chemotaxis and a reduction in cell spreading, adhesion, and lamellipodial extensions. Our previous study also indicated that p57/coronin-1 and F-actin transiently accumulated in phagocytic cups and phagosomal membranes during phagocytosis in neutrophils and neutrophil-like differentiated HL60 cells (15, 16). The transient association of p57/coronin-1 with phagosomes is thought to be closely related to the fusion of phagosomes and lysosomes, because phagolysosomes form immediately after the dissociation of p57/coronin-1 from phagosomes. Ferrari *et al.* (17) demonstrated the relevance of p57/coronin-1 to intracellular parasitism of *Mycobacterium tuberculosis* in murine macrophages by showing that the failure of lysosomes to fuse with phagosomes containing mycobacteria was accompanied by the prolonged accumulation of p57/coronin-1 around the phagosomes. Recently, their group also showed the involvement of p57/coronin-1 in the Ca^{2+}-dependent signaling processes leading to phagosome-lysosome fusion upon mycobacterial infection (18). These results strongly suggest that p57/coronin-1 plays a crucial role in regulating the formation and maturation of phagosomes.

* This study was supported by the Ministry of Education, Culture, Sports, Science, and Technology of Japan and by the Open Research Center Project. The costs of publication of this article were defrayed in part by the payment of page charges. This article must therefore be hereby marked "*advertisement*" in accordance with 18 U.S.C. Section 1734 solely to indicate this fact.

[1] To whom correspondence should be addressed: Dept. of Microbiology, Hoshi University School of Pharmacy and Pharmaceutical Sciences, 2-4-41 Ebara, Shinagawa-ku, Tokyo 142-8501, Japan. Fax: 81-3-5498-5753; E-mail: tsuji@hoshi.ac.jp.

We previously reported that p57/coronin-1 was phosphorylated in neutrophil-like differentiated HL60 cells concomitantly with the dissociation of p57/coronin-1 from phagosomes after the cells phagocytosed opsonized zymosan (16). Purified p57/coronin-1 was also found to be phosphorylated at serine residues by protein kinase C (PKC)[2] *in vitro*. Furthermore, the dissociation of p57/coronin-1 from F-actin surrounding phagosomes was impaired by PKC inhibitors (16). These results implicate p57/coronin-1 phosphorylation in the intracellular localization of this actin-binding protein. Thus, we postulated that the association of p57/coronin-1 with phagosomes via actin filaments is regulated by PKC-dependent phosphorylation of p57/coronin-1 during phagocytosis. In this study we present evidence that the phosphorylation of p57/coronin-1 is enhanced by a PKC activator, phorbol 12-myristate 13-acetate (PMA), and down-regulates the association of p57/coronin-1 with F-actin.

MATERIALS AND METHODS

Reagents—Restriction endonucleases, modifying enzymes, and calf intestine alkaline phosphatase were purchased from TaKaRa (Osaka, Japan) and Toyobo (Osaka, Japan). Hybond-ECL™ nitrocellulose membranes, Immobiline™ DryStrip, and IPG buffer were products of GE Healthcare. Calyculin A, chelerythrine chloride, Triton X-100, 1,4-diazabicycle-2,2,2-octane, rhodamine-conjugated phalloidin, and actin (from rabbit muscle) were purchased from Sigma. Nonidet P-40 and dithiothreitol were from Nacalai Tesque (Kyoto, Japan) and Roche Diagnostics, respectively. Latrunculin B was purchased from Biomol (Plymouth Meeting, PA). CHAPS, PMA, and iodoacetamide were purchased from Wako Pure Chemical (Osaka, Japan). Oligonucleotides were supplied by Hokkaido System Science (Sapporo, Japan).

Antibodies—A monoclonal antibody against human p57/coronin-1 (N7) that recognizes the C-terminal region of the molecule was prepared in our laboratory (15). Anti-actin antibody was purchased from Sigma. Horseradish peroxidase-conjugated goat antibodies to mouse IgG and rabbit IgG were purchased from Kirkegaard & Perry Laboratories (Gaithersburg, MD) and Caltag Laboratories (Burlingame, CA), respectively. Alexa Fluor 488-conjugated goat anti-mouse IgG was from Invitrogen.

DNA Constructs—A construct for a fusion protein of full-length p57/coronin-1 (p57FL) with enhanced green fluorescent protein (EGFP) at the N terminus of p57/coronin-1 (pEGFP-p57FL) was prepared by PCR using a set of primers (sense, 5′-GGG GAA TTC AGA ATG AGC CGG CAG GTG G-3′; antisense, 5′-GGG GAA TTC AAG CTT GGG GCT CTA CTT GGC CTG G-3′) followed by digestion with EcoRI and subcloning in a pEGFP-C2 vector (BD Bioscience Clontech). The cDNA for the truncated form of p57/coronin-1 in a pEGFP-C2 vector (pEGFP-p57LZ; amino acid residues 372–461, including a coiled-coil domain with a leucine zipper motif) was prepared as described previously (12). The nucleotide sequences of these clones were confirmed with a DNA sequencer (Applied Biosystems, Foster City, CA) using the dye-terminator method.

Cell Culture and Transfection—HL60, COS-1, and HEK293T cells were grown in RPMI1640 medium (Invitrogen) supplemented with 10% heat-inactivated fetal calf serum (HyClone, Logan, UT) at 37 °C under humidified 5% CO_2. HEK293T, COS-1, and HL60 cells with EGFP-tagged p57/coronin-1 constructs were transfected by electroporation (Gene Pulsar Xcell™, Bio-Rad) as described previously (12). Briefly, 30 μg of plasmid DNA was added to the cell suspension (3.5×10^6 cells for HEK293 and COS-1 cells in 0.7 ml of phosphate-buffered saline (PBS) and 5×10^6 cells in 0.2 ml of RPMI1640 medium, 10% fetal calf serum for HL60 cells). The mixture was transferred into a 0.4-cm electrode gap electroporation cuvette and subjected to a single pulse of 300 V at a capacitance of 975 microfarads. The cell suspension was then diluted with 10 ml of RPMI1640 medium, 10% fetal calf serum and cultured at 37 °C for 24–48 h. Stable transfectants of HEK293T cells were cloned by the limiting dilution.

Electrophoresis and Immunoblotting—SDS-PAGE and immunoblotting were conducted as described previously (12).

Isolation of the Cytoskeleton-rich Fraction—The cytoskeleton-containing detergent-insoluble fraction was isolated according to the method of Gatfield *et al.* (19). Cell pellets (1×10^6 cells) were suspended in 0.3 ml of ice-cold cytoskeleton isolation buffer (80 mM PIPES, pH 6.8, containing 5 mM EGTA, 1 mM $MgCl_2$, and 1% Triton X-100). The suspension was immediately centrifuged at $5000 \times g$ for 3 min to obtain the detergent-insoluble cytoskeleton-containing fraction and the detergent-soluble cytosolic fraction. The cells were treated with or without the following reagents at 37 °C for 30 min before extraction with the cytoskeleton isolation buffer: PMA (150 nM) and calyculin A (100 nM) for PKC activation, chelerythrine (30 μM) for PKC inhibition, or latrunculin B (5 μM) for inhibition of actin polymerization (for depolymerization of F-actin).

Fluorescence Microscopy—The intracellular distribution of p57/coronin-1 and F-actin in HL60 cells was observed by immunofluorescence microscopy. Cells were treated with the cytoskeleton isolation buffer at 4 °C for 3 min, washed with PBS once, fixed with 3.8% neutral buffered formaldehyde at 4 °C for 10 min, and incubated with anti-p57/coronin-1 antibody (5 μg/ml) in PBS containing 3% bovine serum albumin for 60 min. After washing 3 times with PBS, the cells were incubated with Alexa Fluor 488-conjugated anti-mouse IgG (dilution 1:200) and rhodamine-conjugated phalloidin (15 units/ml) in PBS containing 3% bovine serum albumin for 30 min. The labeled cells thus prepared were washed 3 times with PBS and then mounted on a slide glass with 2.3% 1,4-diazabicycle-2,2,2-octane, 90% glycerol.

COS-1 and HEK293T cells that had been transfected with plasmids containing a gene for EGFP were cultured on a Lab-Tek II Chamber Slide (Nalge Nunc, Rochester, NY) at 37 °C for 48 h. Fluorescently labeled cells were observed using a confocal laser-scanning microscope (Radiance 2100, Bio-Rad; LSM5 Exciter, Carl Zeiss MicroImaging Co., Ltd.). Fluorescence in the green and red channels was visualized with 488 nm (argon laser) and 543 nm (helium/neon laser) laser lines, respectively.

[2] The abbreviations used are: PKC, protein kinase C; CHAPS, 3-[(3-cholamidopropyl)-dimethylammonio]propanesulfonic acid; ECL, enhanced chemiluminescence; EGFP, enhanced green fluorescent protein; F-actin, filamentous actin; PBS, phosphate-buffered saline; PMA, phorbol 12-myristate 13-acetate; PIPES, 1,4-piperazinediethanesulfonic acid.

Images were collected under non-saturating conditions set up by the use of an output LUT (look-up table).

Two-dimensional Gel Electrophoresis—HL60 cells (1×10^6 cells) were washed with cold PBS and incubated with 0.3 ml of lysis buffer (50 mM Tris-HCl, pH 7.5, containing 150 mM NaCl, 1 mM EDTA, and 1% Nonidet P-40) at 4 °C for 10 min. The cell lysate was centrifuged at 15,000 × *g* for 15 min, and the supernatant was diluted with 9 volumes of rehydrating buffer (7 M urea, 2 M thiourea, 4% CHAPS, 40 mM dithiothreitol, 0.5% IPG buffer (pH 4–7 or 5.5–6.7), and 0.002% bromphenol blue). Immobiline™ DryStrips (7 cm, pH 4–7 or 5.3–6.5) were incubated with the diluted cell lysate and rehydrated for 12 h at 20 °C. The protein-loaded strip was then subjected to isoelectric focusing (IEF) (CoolPhoreStar IPG-IEF Type-P, Anatech, Tokyo, Japan). Isoelectric focusing was conducted under the following conditions: 500 V for 1 h, 700 V for 15 min, 1000 V for 15 min, 1500 V for 15 min, 2000 V for 15 min, 2500 V for 15 min, 3000 V for 15 min, and 3500 V for 4 h. After the proteins were separated by isoelectric focusing, the strips were incubated for 10 min in equilibration buffer (50 mM Tris-HCl, pH 8.8, 6 M urea, 1% SDS, 30% glycerol, and 0.002% bromphenol blue) containing 0.25% dithiothreitol and subsequently for 10 min in the same buffer containing 4.5% iodoacetamide. The proteins in the strips were then electrophoresed on 10% polyacrylamide gels (second dimension) and electrically transferred onto a nitrocellulose membrane. The membrane was treated with monoclonal anti-p57/coronin-1 antibody followed by horseradish peroxidase-conjugated anti-mouse IgG antibody. The proteins were visualized by an enhanced chemiluminescence (ECL) detection system (GE Healthcare) according to the manufacturer's instructions.

Co-sedimentation Assay with F-actin—HL60 cells (3×10^6 cells) were suspended in ice-cold G-actin buffer (5 mM Tris-HCl, pH 8.0, 0.2 mM $CaCl_2$, 0.2 mM ATP, and 1 mM dithiothreitol) and homogenized with 30 strokes in a Dounce homogenizer (tight-fitting). After the homogenate was centrifuged at 200,000 × *g* for 60 min, the supernatant was mixed with a 1/9 volume of 10× actin polymerizing solution (final concentration: 50 mM KCl, 2 mM $MgCl_2$, 1 mM ATP) and actin (5 μg), and the mixture was incubated at 25 °C for 120 min to allow polymerization of G-actin. The reaction mixture was centrifuged at 200,000 × g for 60 min, and the supernatant and precipitate were analyzed by one- and two-dimensional gel electrophoresis and immunoblotting.

Affinity Chromatography of p57/Coronin-1—HL60 cells (2.5×10^8 cells) that had been treated with or without PMA (150 nM) and calyculin A (100 nM) at 37 °C for 30 min were incubated with lysis buffer at 4 °C for 10 min, and the cell lysate was centrifuged at 18,000 × *g* for 15 min. The supernatant obtained was applied to a column of anti-p57/coronin-1 antibody-conjugated Sepharose (12). After unbound materials washed with PBS, p57/coronin-1 bound to the column was eluted with 0.1 M glycine-HCl buffer, pH 2.7. The eluate was immediately neutralized by adding a 1/9 volume of 1 M Tris-HCl buffer, pH 9.0, and an aliquot was analyzed by SDS-PAGE and immunoblotting. For the detection of p57/coronin-1, the silver staining method (two-dimensional silver stain II kit, Daiichi Pure Chemical, Tokyo, Japan) was conducted according to the manufacturer's protocol. Actin that was co-purified with p57/coronin-1 was detected by immunoblotting using anti-actin antibody and horseradish peroxidase-conjugated anti-rabbit IgG antibody followed by the ECL detection system (GE Healthcare).

Phagocytosis of IgG-coated Magnetic Beads—Human IgG (Sigma) was bound to Dynabeads M-270 carboxylic acid (3.0 μm; Invitrogen) according to the manufacturer's instructions. The IgG-coated beads were then opsonized with normal human serum (blood group AB, Sigma) for 30 min at 37 °C and washed twice with PBS. HL60 cells were differentiated in PRMI1640 medium containing 10% fetal calf serum and 1.25% dimethyl sulfoxide for 5 days, and neutrophil-like differentiated HL60 cells (4×10^6 cells) were incubated with opsonized Dynabeads at 37 °C for 5–30 min. The cells phagocytosing Dynabeads were magnetically enriched, and the cytoskeleton-containing detergent-insoluble fraction was isolated as described above.

RESULTS

Association of p57/Coronin-1 with the Actin Cytoskeleton—We first examined the association of p57/coronin-1 with the actin cytoskeleton in HL60 human leukemic cells. To enrich the actin cytoskeleton, the cells were extracted with cytoskeleton isolation buffer containing 1% Triton X-100 followed by centrifugation 5000 × *g* for 3 min. The actin-containing cytoskeleton was reported to be recovered in the precipitate fraction after these procedures (19). When the supernatant and the precipitate fractions after centrifugation were analyzed by SDS-PAGE and immunoblotting, a major part of p57/coronin-1 was recovered in the detergent-insoluble F-actin-rich fraction (Fig. 1*A*). We next microscopically observed the intracellular distribution of p57/coronin-1 and F-actin by using anti-p57/coronin-1 antibody and rhodamine-conjugated phalloidin, respectively. After HL60 cells were treated with cytoskeleton isolation buffer and fluorescently labeled with these reagents, the cells were observed using a confocal laser-scanning microscope. As shown in Fig. 1*B*, p57/coronin-1 was localized at the cell periphery showing a quite similar distribution of F-actin. We then examined the effect of latrunculin B, an F-actin-depolymerizing reagent (20), on the co-localization of p57/coronin-1 with the cytoskeleton. Disruption of the actin cytoskeleton by the treatment of HL60 cells with latrunculin B (5 μM) at 37 °C for 30 min before cell lysis decreased the recovery of p57/coronin-1 in the detergent-insoluble fraction (Fig. 1*C*), concomitant with a lower yield of actin in the precipitate fraction.

Our previous study indicated that p57/coronin-1 possessed at least two actin binding sites in the N-terminal region (11). To examine the role of the putative actin-binding regions of the molecule in its association with the actin cytoskeleton, we prepared two constructs in which the full-length p57/coronin-1 (p57FL) and the C-terminal portion of p57/coronin-1 (p57LZ) cDNA were ligated with a vector containing the enhanced EGFP gene. The p57LZ construct lacks two putative actin binding regions but contains the leucine zipper motif in the coiled-coil domain, as schematically shown in Fig. 2*A*. The chimeric fusion proteins (EGFP-p57FL and EGFP-p57LZ) were expressed in HEK293T cells, and the intracellular distribution of these proteins in the transfected cells was observed under fluorescence microscopy. EGFP-p57FL was localized in the

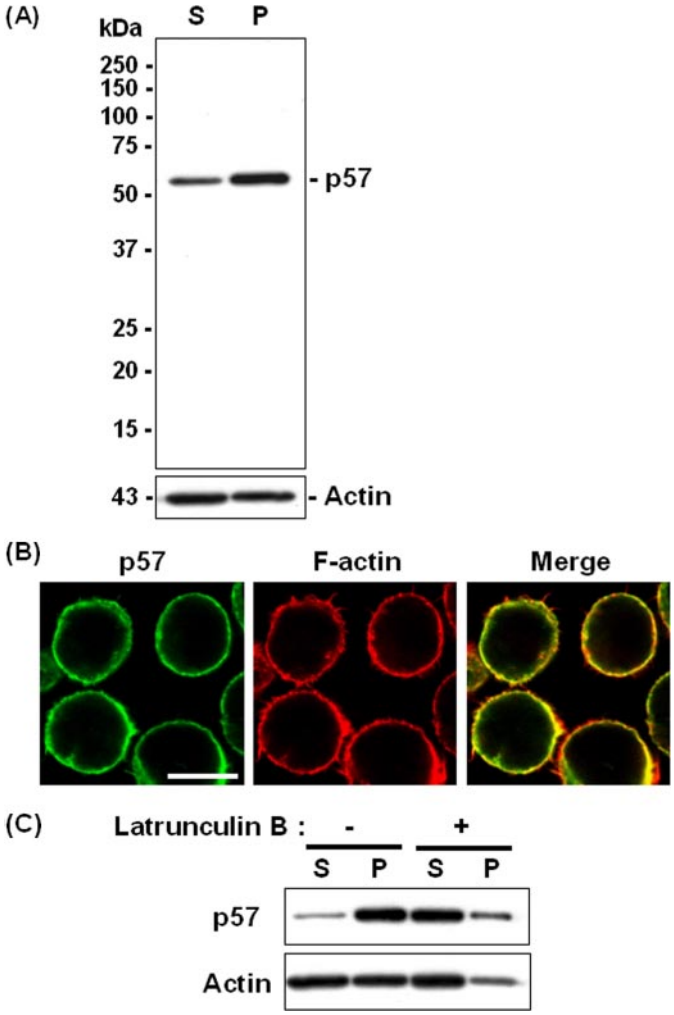

FIGURE 1. **Association of p57/coronin-1 with the actin cytoskeleton in HL60 cells.** *A*, HL60 cells were lysed with a Triton-X100-containing buffer (cytoskeleton isolation buffer) (12), and the lysate was separated into the detergent-soluble supernatant (*S*) and the detergent-insoluble precipitate (*P*) by centrifugation. These fractions were analyzed by SDS-PAGE and immunoblotting using anti-p57/coronin-1 and anti-actin antibodies. *B*, the intracellular distribution of p57/coronin-1 and F-actin in HL60 cells that had been treated with cytoskeleton isolation buffer was observed under a confocal laser-scanning microscope. *Scale bar* = 5 μm. *C*, HL60 cells were treated with 5 μM latrunculin B for 30 min. The actin cytoskeleton and cytosol fractions were separated from these cells by the extraction with cytoskeleton isolation buffer followed by centrifugation and analyzed by SDS-PAGE and immunoblotting using anti-p57/coronin-1 and anti-actin antibodies.

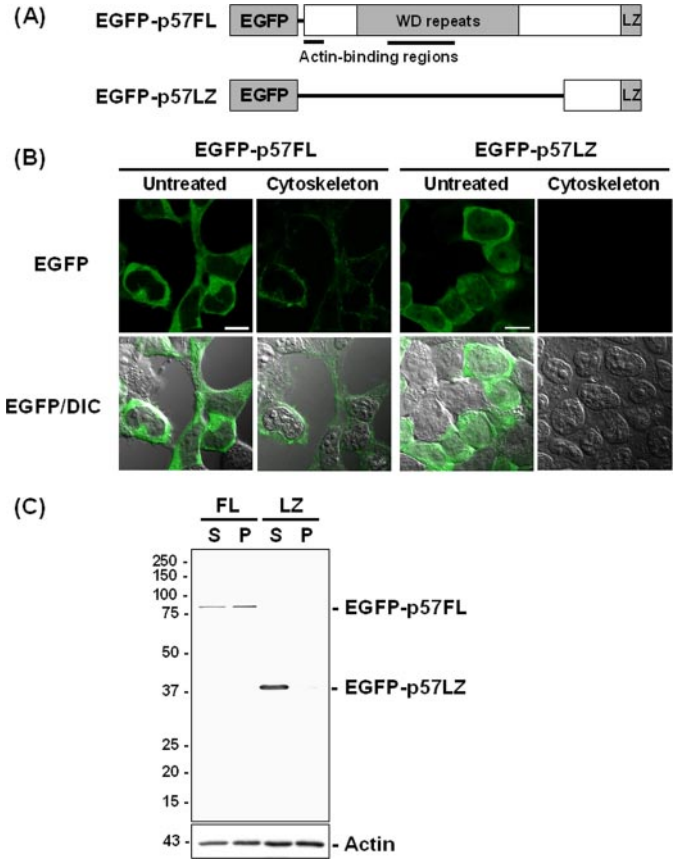

FIGURE 2. **Association of EGFP-p57FL, but not EGFP-p57LZ, with the actin cytoskeleton.** *A*, schematic diagrams of the structures of EGFP-p57FL (an EGFP fusion protein with the full-length of p57/coronin-1) and EGFP-p57LZ (an EGFP fusion protein with the C-terminal region of p57/coronin) are shown. *LZ*, leucine zipper motif. *B*, EGFP-p57FL (*left panels*) and EGFP-p57LZ (*right panels*) were stably expressed in HEK293T cells, and these transfectant cells were observed under a confocal laser scanning microscope. Before the microscopic observation, these cells were extracted with (*Cytoskeleton*) or without (*Untreated*) cytoskeleton isolation buffer for 1 min. The fluorescence images are superimposed with differential interference contrast images (*EGFP/DIC*, *lower panels*). *Scale bars* = 10 μm. *C*, the transfectant cells were extracted with cytoskeleton isolation buffer, and the lysate was separated by centrifugation at 5000 $\times$ *g* for 3 min. The soluble cytosol fraction (*S*) and insoluble actin cytoskeleton fraction (*P*) were analyzed by SDS-PAGE/immunoblotting using anti-p57/coronin-1 antibody. *FL*, EGFP-p57FL; *LZ*, EGFP-p57LZ.

peripheral cortex region, whereas EGFP-p57LZ was rather diffusely distributed within a whole cell (Fig. 2*B*). After these cells were extracted with cytoskeleton isolation buffer, EGFP-p57FL was still present at least in part in the cell periphery, whereas EGFP-p57LZ was almost completely abolished. Furthermore, the analysis by SDS-PAGE/immunoblotting indicated that EGFP-p57FL was detected in both the detergent-soluble and insoluble fractions but also that EGFP-p57LZ was recovered exclusively in the detergent-soluble fraction (Fig. 2*C*). These results suggest that the association of p57/coronin-1 with the actin cytoskeleton depends on the presence of the putative actin binding sites located in the N-terminal region.

Effects of PMA Stimulation on the Intracellular Distribution of p57/Coronin-1—In the previous study we reported that p57/coronin-1 was phosphorylated upon the treatment of HL60 cells with PMA and that the phosphorylation of p57/coronin-1 was abrogated by inhibitors for PKC (16). We, therefore, examined the possible roles of p57/coronin-1 phosphorylation in its functions, such as binding capacity to the actin cytoskeleton. The actin cytoskeleton was isolated from HL60 cells that had been treated with PMA or chelerythrine, a pan-PKC inhibitor, and its interaction with p57/coronin-1 was analyzed. When the cells were stimulated with PMA, the distribution of p57/coronin-1 to the detergent-soluble fraction was increased in parallel with a decrease in that of the detergent-insoluble fraction (Fig. 3*A*). In contrast, the recovery of p57/coronin-1 in the detergent-insoluble fraction was slightly increased when the cells were pretreated with chelerythrine. The stimulation with PMA of chelerythrine-pretreated cells gave essentially the same result.

Fluorescence microscopic observations of PMA-treated HL60 cells also demonstrated that the distribution of p57/coronin-1 to the cell periphery was clearly decreased upon PMA

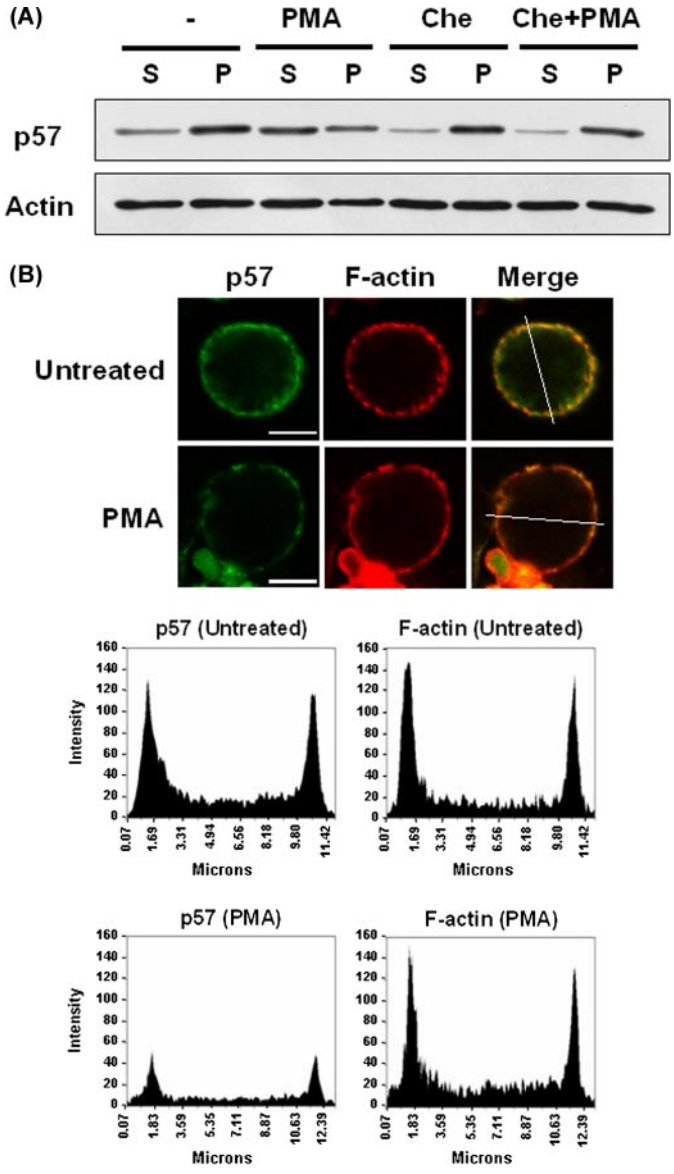

FIGURE 3. **Effects of PMA and chelerythrine on the intracellular distribution of p57/coronin-1.** *A*, HL60 cells were treated with PMA (150 nM), chelerythrine (*Che*, 30 μM), or chelerythrine plus PMA at 37 °C for 30 min and lysed with cytoskeleton isolation buffer. The lysate was centrifuged at 3000 × *g* for 3 min to recover the cytosol fraction (supernatant (*S*)) and the actin cytoskeleton fraction (precipitate (*P*)). These fractions were analyzed by SDS-PAGE and immunoblotting using anti-p57/coronin-1 and anti-actin antibodies. *B*, HL60 cells that had been treated with or without PMA were extracted with cytoskeleton isolation buffer. The cells, thus, treated were stained with anti-p57/coronin-1 and Alexa Fluor 488-conjugated anti-mouse IgG antibodies (*green*) and rhodamine-conjugated phalloidin (*red*) and observed under a confocal laser scanning microscope (*upper panels*). *Scale bars* = 5 μm. The fluorescence intensity of the cross-section of each image, which is indicated in the *upper panels*, was quantified by using LaserSharp software (Bio-Rad) (*lower panels*).

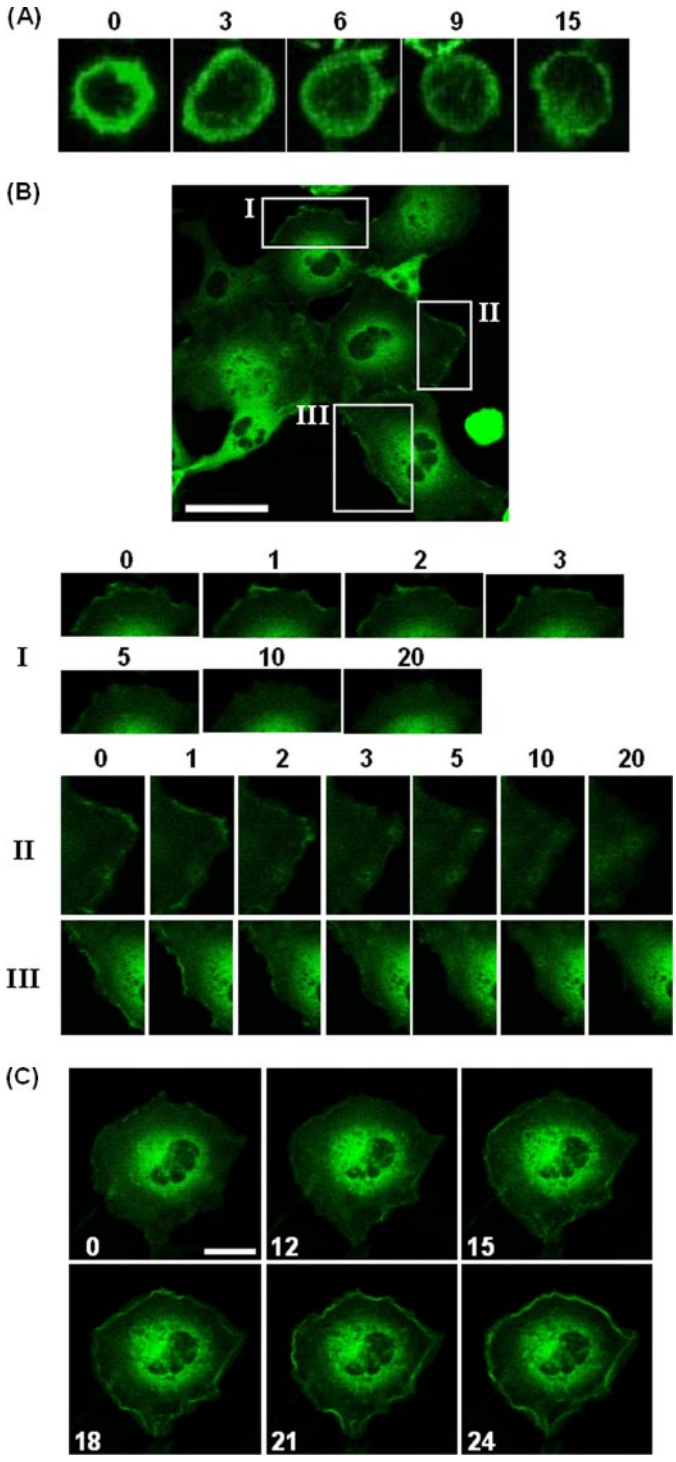

FIGURE 4. **Effects of PMA and chelerythrine on the intracellular distribution of EGFP-p57FL.** Living HL60 and COS-1 cells transiently expressing EGFP-p57FL were monitored by confocal time-lapse microscopy. Time in this figure is indicated in minutes after treatment with PMA or chelerythrine. *A*, HL60 cells expressing EGFP-p57FL were placed on a poly-L-lysine-coated slide glass and stimulated with PMA (150 nM). *B*, COS-1 cells expressing EGFP-p57FL were stimulated with PMA (150 nM). *Scale bar* = 50 μm. Magnified views of boxed regions I–III appear in the *lower panels*. *C*, COS-1 cells expressing EGFP-p57FL were treated with chelerythrine (30 μM). *Scale bar* = 20 μm.

treatment without significant change in F-actin distribution (Fig. 3*B*, *upper panels*). The decrease in the distribution of p57/coronin-1 to the actin-rich cortical region after PMA treatment was confirmed by quantitative analysis of fluorescence intensity in the cross-section of the cell (Fig. 3*B*, *lower panels*). We further conducted time-course analysis of the translocation of EGFP-p57FL in transiently transfected HL60 cells after treatment with PMA. EGFP-p57FL fluorescence was originally located in the cell cortical regions and gradually decreased, showing a rather dispersed distribution within 15 min after treatment with PMA (Fig. 4*A*). We also attempted to observe this process in EGFP-p57FL-transfected COS-1 cells, in which cell cortex regions can be observed clearly by virtue of their

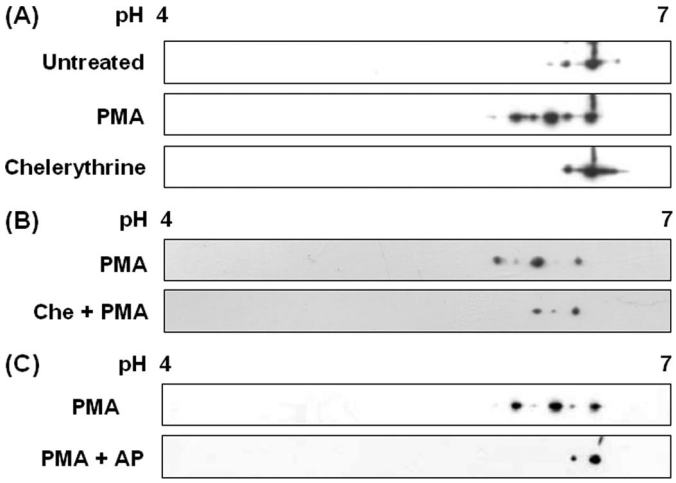

FIGURE 5. **Two-dimensional gel electrophoresis of p57/coronin-1.** The lysate of HL60 cells was subjected to two-dimensional gel electrophoresis and immunoblotting using anti-p57/coronin-1 antibody. *A*, HL60 cells that had been treated with PMA (150 nM) or chelerythrine (*Che*, 30 μM). *B*, the lysate of PMA-treated or chelerythrine plus PMA-treated HL60 cells. *C*, the lysate of PMA-treated HL60 cells followed by incubation with (*PMA + AP*) or without (*PMA*) alkaline phosphatase (50 units/ml) at 37 °C for 120 min.

large cell bodies with well spread morphology (Fig. 4*B*). Similar but more definite results were obtained in transfected COS-1 cells; namely, the fluorescence originally located at the cell periphery gradually decreased, disappearing almost completely 10 min after PMA treatment. In contrast, the treatment of these cells with chelerythrine increased the fluorescence localization in the cell cortex regions in a time-dependent manner (Fig. 4*C*).

Separation of p57/Coronin-1 by Two-dimensional Gel Electrophoresis—We next analyzed the phosphorylation status of p57/coronin-1 derived from PMA-treated, chelerythrine-treated, or chelerythrine plus PMA-treated HL60 cells as well as untreated cells by two-dimensional gel electrophoresis and immunoblotting. From the lysate of untreated HL60 cells, one major spot and one minor spot around pI 6.3 were detected by using anti-p57/coronin-1 antibody (Fig. 5*A*). When the cells were treated with PMA, we found three additional spots in more acidic regions. The chelerythrine-treated HL60 cells gave one major spot and one minor spot, as shown in the case of untreated cells. The pretreatment of the cells with chelerythrine abrogated the effect of PMA (Fig. 5*B*). These results indicate that p57/coronin-1 of HL60 cells are electrically heterogeneous, probably due to different degrees of phosphorylation. To examine whether the heterogeneity in electric charge of p57/coronin-1 was attributable to phosphorylation, the cell lysate was treated with alkaline phosphatase before electrophoretic separation (Fig. 5*C*). The alkaline phosphatase treatment of the cell lysate from PMA-treated HL60 cells eliminated acidic spots to give almost a single spot corresponding to that with the lowest pI. These results strongly suggest that p57/coronin-1 is phosphorylated in at least four sites in a PMA-dependent manner and that the phosphorylation modulates the ability of p57/coronin-1 to bind to the actin cytoskeleton.

Modulation of Actin Binding Capacity of p57/Coronin-1 by Phosphorylation—We subsequently addressed the hypothesis that the phosphorylation of p57/coronin-1 down-regulates its binding to F-actin. The detergent-insoluble F-actin-rich fraction and the detergent-soluble cytosolic fraction were prepared from PMA-stimulated HL60 cells, and the phosphorylation of p57/coronin-1 present in these fractions was analyzed by two-dimensional gel electrophoresis in the pI range of 5.3–6.5. The results of immunoblotting indicated that the cytosolic fraction (supernatant) contained more phosphorylated forms of p57/coronin-1 than did the cytoskeletal fraction (precipitate) (Fig. 6); the phosphorylated forms of p57/coronin-1 in the supernatant and the precipitate were estimated be 72 and 45%, respectively, based on the intensities of the spots on the immunoblotting analysis.

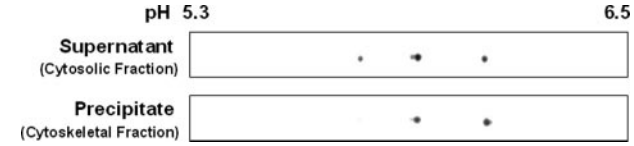

FIGURE 6. **Analysis of p57/coronin-1 associated with the actin cytoskeleton by two-dimensional gel electrophoresis.** PMA-treated HL60 cells were separated into cytosol (*Supernatant*) and cytoskeleton (*Precipitate*) fractions by extraction with cytoskeleton isolation buffer. These fractions were analyzed by two-dimensional gel electrophoresis and immunoblotting using anti-p57/coronin-1 antibody.

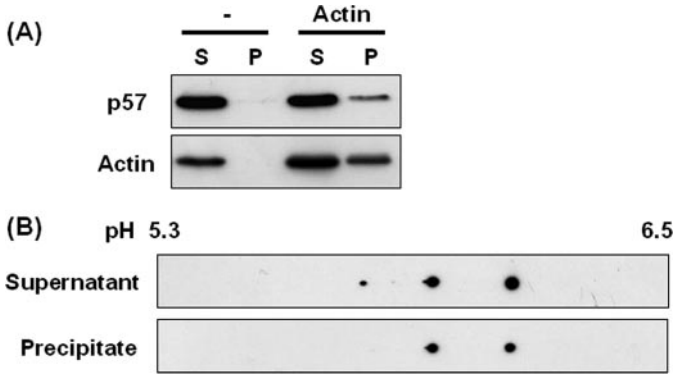

FIGURE 7. **Co-sedimentation of p57/coronin-1 with F-actin.** PMA-treated HL60 cells were homogenized in G-actin buffer and centrifuged at 200,000 × *g* for 60 min to remove insoluble materials. The supernatant was mixed with or without G-actin (5 μg) and then with actin polymerizing solution, and the mixture was incubated at 25 °C for 120 min. After centrifugation at 200,000 × *g* for 60 min, the supernatant and precipitate were analyzed by one- and two-dimensional gel electrophoresis and immunoblotting. *A*, the supernatant (*S*) and precipitate (*P*) were analyzed by SDS-PAGE/immunoblotting using anti-p57/coronin-1 and anti-actin antibodies. *B*, the supernatant and precipitate were analyzed by two-dimensional gel electrophoresis/immunoblotting using anti-p57/coronin-1 antibody.

We next performed a co-sedimentation assay in which we analyzed p57/coronin-1 co-precipitated with F-actin after polymerization and centrifugation. G-actin was polymerized to form F-actin in the presence of the cytosolic fraction prepared from PMA-stimulated HL60 cells, and the reaction mixture was subjected to high speed centrifugation to sediment F-actin. The immunoblotting analysis of the supernatant and the precipitate fractions showed that a portion of the p57/coronin-1 derived from PMA-treated HL60 cells was precipitated with polymerized F-actin (Fig. 7*A*). We compared p57/coronin-1 co-precipitated with F-actin with that remaining in the supernatant after the actin polymerization for their phosphorylated nature. Although both the supernatant and the precipitate fractions gave rather similar profiles in two-dimensional gel electrophoresis, the most acidic spot was detected only for p57/coronin-1 from the cytosolic fraction (Fig. 7*B*).

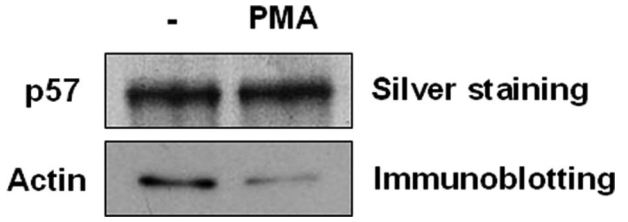

FIGURE 8. **Association of actin with p57/coronin-1 purified by affinity chromatography.** The lysate of PMA-treated or untreated HL60 cells was applied to a column of anti-p57/coronin-1 antibody-conjugated Sepharose as described under "Materials and Methods." The fraction bound to and eluted from the column was analyzed by SDS-PAGE and immunoblotting using anti-p57/coronin-1 antibody. The p57/coronin-1 and actin co-purified with p57/coronin-1 were detected by silver staining and by immunoblotting with anti-actin antibody, respectively. The bands for actin were visualized with horseradish peroxidase-conjugated secondary antibody and the ECL detection system (GE Healthcare).

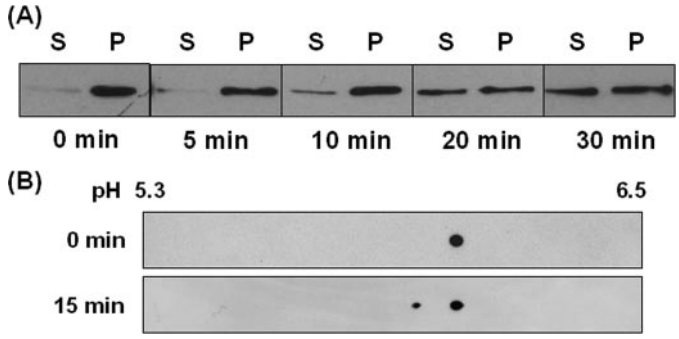

FIGURE 9. **Intracellular localization and phosphorylation of p57/coronin-1 in phagocytosing cells.** *A*, differentiated HL60 cells were incubated with opsonized Dynabeads at 37 °C for 5–30 min. Phagocytosing cells were magnetically enriched and then extracted with cytoskeleton isolation buffer. After centrifugation at 3000 × *g* for 3 min, the supernatant (cytosol fraction) (*S*) and the precipitate (actin cytoskeleton fraction) (*P*) were analyzed by SDS-PAGE and immunoblotting using anti-p57/coronin-1 antibody. *B*, the lysate of phagocytosing cells was analyzed by two-dimensional gel electrophoresis and immunoblotting using anti-p57/coronin-1 antibody.

The association of p57/coronin-1 with actin was also assessed by affinity chromatography using a column of anti-p57/coronin-1 antibody-conjugated Sepharose as described previously (12). The lysate of HL60 cells that had been treated with or without PMA was applied to the affinity column, and the proteins bound by the column were analyzed by SDS-PAGE followed by silver staining for p57/coronin-1 and immunoblotting for actin. As shown in Fig. 8, the amount of actin co-purified with p57/coronin-1 was decreased after HL60 cells were stimulated with PMA, although similar amounts of p57/coronin-1 were bound to and eluted from the column. Taken together, these results strongly suggest that the phosphorylation of p57/coronin-1 negatively regulates its association with the actin cytoskeleton.

Intracellular Localization and Phosphorylation of p57/Coronin-1 during Phagocytosis—We finally examined the possible relationship between the intracellular distribution and phosphorylation level of p57/coronin-1 during phagocytosis in neutrophil-like differentiated HL60 cells. Differentiated HL60 cells phagocytosing IgG-coated Dynabeads were separated into detergent-insoluble cytoskeleton-rich and detergent-soluble cytosolic fractions, and the distribution of p57/coronin-1 in these fractions was analyzed by immunoblotting. As shown in Fig. 9*A*, the amounts of p57/coronin-1 associated with the cytoskeleton decreased during the phagocytotic process, and this protein was distributed almost equally in both fractions 20 min after the initiation of phagocytosis. Two-dimensional electrophoresis revealed that the lysate prepared from cells phagocytosing beads for 15 min contained a phosphorylated form of p57/coronin-1 that was not observed in the lysate from non-phagocytosing cells (Fig. 9*B*). This result is consistent with our previous observation that the incorporation of ^{32}P into p57/coronin-1 increased at a late phase of zymosan phagocytosis of [^{32}P]phosphate-labeled differentiated HL60 cells (16).

DISCUSSION

In the present study we characterized the phosphorylation of p57/coronin-1 and its role in regulating the association of this protein with the actin cytoskeleton. The supposition that phosphorylation attenuates the interaction between p57/coronin-1 and F-actin is based on the following results. 1) PMA treatment of HL60 cells or p57/coronin-1-transfected COS-1 cells decreased the association of p57/coronin-1 with the cytoskeletal fraction as assessed by SDS-PAGE/immunoblotting, in parallel with the reduction of the co-localization of p57/coronin-1 with actin filaments under microscopic observation (Figs. 3 and 4). 2) The p57/coronin-1 molecules associated with the actin cytoskeleton in HL60 cells, and those co-sedimented with F-actin polymerized *in vitro* were phosphorylated at lower levels than the molecules not associated with the actin filaments (Figs. 6 and 7). 3) p57/coronin-1 purified from PMA-treated HL60 cells showed lower affinity for actin than that purified from untreated HL60 cells (Fig. 8). The regulatory mechanism underlying the interaction between p57/coronin-1 and actin filaments seems to be of considerable importance, because the intracellular localization of this actin-binding protein changes during various actin-dependent cellular processes, including phagocytosis. Our experiment using neutrophil-like differentiated HL60 cells indeed indicated that p57/coronin-1 was dissociated from the actin cytoskeleton during phagocytosis of opsonized particles in association with phosphorylation of this molecule (Fig. 9). The phosphorylation/dephosphorylation of p57/coronin-1 appears to be regulated more actively in phagocytosing cells than in quiescent cells. The results obtained in this study may explain our previous observation that the dissociation of p57/coronin-1 transiently accumulated in phagosomes in neutrophils was impaired by treating the cells with PKC inhibitors (16). The dissociation of p57/coronin-1 from F-actin-coated phagosomes is thought to be indispensable for phagosome-lysosome fusion, and PKC-dependent protein phosphorylation may be involved in this process (16–18). It is most likely that the dissociation of non-phosphorylated forms of p57/coronin-1 that cross-link F-actin associated with phagosomal membranes is triggered by phosphorylation catalyzed directly or indirectly by PKC. Thus, the phosphorylation of p57/coronin-1 appears to be important for the late phase of phagosome maturation.

M. tuberculosis is known as an intracellular parasite that survives in phagosomes after being phagocytosed in macrophages accompanying the sustained accumulation of p57/coronin-1 on phagosomes containing mycobacteria (17). *M. tuberculosis* might escape attack from the host immune system by inhibiting

the phosphorylation or enhancing the dephosphorylation of p57/coronin-1. It was reported that *M. tuberculosis* secreted phosphatases called MptpA and MptpB (21) and that these phosphatases were closely related to the virulence and the intracellular parasitism (22). However, considering that these phosphatases are tyrosine phosphatases (21), they are unlikely to be implicated in the dephosphorylation of p57/coronin-1 because p57/coronin-1 is phosphorylated at serine residues (16). A recent study by Jayachandran *et al.* (18) of mice deficient in p57/coronin-1 demonstrated that p57/coronin-1 was dispensable for the early phase of phagocytosis but was required for regulating lysosomal delivery of mycobacteria through the activation of the Ca^{2+}-dependent phosphatase, calcineurin. In p57/coronin-1-deficient macrophages, therefore, the phagosome-lysosome fusion was not impaired, resulting in the killing of mycobacteria. Their study suggests a novel function of p57/coronin-1 in the Ca^{2+}-dependent cellular signaling processes.

Two-dimensional gel electrophoresis revealed two major and two minor spots of phosphorylated forms of p57/coronin-1 from PMA-treated HL60 cells (Fig. 5), suggesting that this protein possesses at least four potential phosphorylation sites. In the lysate of untreated HL60 cells, however, the non-phosphorylated forms were predominant. Similar results were obtained when we analyzed human neutrophils, human leukemic cell lines (THP-1, U937, and Jurkat), and murine RAW264.7 macrophage-like cells.[3] In contrast, a large portion of the murine counterpart of p57/coronin-1 from the J774A.1 macrophage-like cell line was reported to be phosphorylated (19). The phosphorylation status of this actin-binding protein might depend on the cell type and species. It is highly probable that PKC is involved in the phosphorylation of the p57/coronin-1 molecule, but the phosphorylation sites have not been identified. Recently, Cai *et al.* (23) reported that PKC phosphorylated coronin-2 (also referred to as coronin-1B), a ubiquitously expressed member of the coronin family, and that the major phosphorylation site was Ser-2 of the molecule. The phosphorylation at this site was found to be involved in the regulation coronin-2 binding to actin-related protein complex 2/3 (Arp2/3) as well as in PMA-induced membrane ruffling and cell motility of fibroblasts. Our preliminary experiment using mass spectrometry indicated that Ser-2 of p57/coronin-1 is also phosphorylated, but we obtained no evidence so far showing that the phosphorylation at this site plays a role in regulating its actin binding activity. More recently, Foger *et al.* (24) reported that p57/coronin-1 regulated chemokine-mediated migration of mouse T lymphocyte via an Arp2/3-dependent mechanism. Because the Arp2/3 complex is a key component for the formation of the actin filament networks, it is likely that the association of coronins to the Arp2/3 complex disturbs the rearrangement of the actin cytoskeleton through the inhibition of Arp2/3 complex activity. These studies, including ours, suggest that the phosphorylation of the coronin family of proteins is crucial for regulating the interactions between actin and various actin-associated proteins and that these interactions dynamically control the rearrangement of the actin networks and related cellular functions. The phosphorylation site(s) of p57/coronin-1 involved in the regulation of binding to actin filaments and the roles of the p57/coronin-1 phosphorylation in the reorganization of actin filaments are important issues remaining to be elucidated.

[3] T. Oku, Y. Kaneko, K. Murofushi, Y. Seyama, S. Toyoshima, and T. Tsuji, unpublished observation.

Acknowledgments—We thank Manami Sato, Akime Miyasato, Yoshinori Shinohara, Mariko Takakura, and Kyoko Kobayashi for excellent technical assistance.

REFERENCES

1. de Hostos, E. L., Bradtke, B., Lottspeich, F., Guggenheim, R., and Gerisch, G. (1991) *EMBO J.* **10,** 4097–4104
2. Gerisch, G., Albrecht, R., Heizer, C., Hodgkinson, S., and Maniak, M. (1995) *Curr. Biol.* **5,** 1280–1285
3. de Hostos, E. L., Rehfuess, C., Bradtke, B., Waddell, D. R., Albrecht, R., Murphy, J., and Gerisch, G. (1993) *J. Cell Biol.* **120,** 163–173
4. Maniak, M., Rauchenberger, R., Albrecht, R., Murphy, J., and Gerisch, G. (1995) *Cell* **83,** 915–924
5. Fukui, Y., de Hostos, E. L., and Inoue, S. (1997) *Biol. Bull.* **193,** 224–225
6. Hacker, U., Albrecht, R., and Maniak, M. (1997) *J. Cell Sci.* **110,** 105–112
7. Fukui, Y., Engler, S., Inoue, S., and de Hostos, E. L. (1999) *Cell Motil. Cytoskeleton* **42,** 204–217
8. de Hostos, E. L. (1999) *Trends Cell Biol.* **9,** 345–350
9. Uetrecht, A. C., and Bear, J. E. (2006) *Trends Cell Biol.* **16,** 421–426
10. Suzuki, K., Nishihata, J., Arai, Y., Honma, N., Yamamoto, K., Irimura, T., and Toyoshima, S. (1995) *FEBS Lett.* **364,** 283–288
11. Oku, T., Itoh, S., Okano, M., Suzuki, A., Suzuki, K., Nakajin, S., Tsuji, T., Nauseef, W. M., and Toyoshima, S. (2003) *Biol. Pharm. Bull.* **26,** 409–416
12. Oku, T., Itoh, S., Ishii, R., Suzuki, K., Nauseef, W. M., Toyoshima, S., and Tsuji, T. (2005) *Biochem. J.* **387,** 325–331
13. Yan, M., Di Ciano-Oliveira, C., Grinstein, S., and Trimble, W. S. (2007) *J. Immunol.* **178,** 5769–5778
14. Yan, M., Collins, R. F., Grinstein, S., and Trimble, W. S. (2005) *Mol. Biol. Cell* **16,** 3077–3087
15. Allen, L. A., DeLeo, F. R., Gallois, A., Toyoshima, S., Suzuki, K., and Nauseef, W. M. (1999) *Blood* **93,** 3521–3530
16. Itoh, S., Suzuki, K., Nishihata, J., Iwasa, M., Oku, T., Nakajin, S., Nauseef, W. M., and Toyoshima, S. (2002) *Biol. Pharm. Bull.* **25,** 837–844
17. Ferrari, G., Langen, H., Naito, M., and Pieters, J. (1999) *Cell* **97,** 435–447
18. Jayachandran, R., Sundaramurthy, V., Combaluzier, B., Mueller, P., Korf, H., Huygen, K., Miyazaki, T., Albrecht, I., Massner, J., and Pieters, J. (2007) *Cell* **130,** 37–50
19. Gatfield, J., Albrecht, I., Zanolari, B., Steinmetz, M. O., and Pieters, J. (2005) *Mol. Biol. Cell* **16,** 2786–2798
20. Spector, I., Shochet, N. R., Blasberger, D., and Kashman, Y. (1989) *Cell Motil. Cytoskeleton* **13,** 127–144
21. Koul, A., Choidas, A., Treder, M., Tyagi, A. K., Drlica, K., Singh, Y., and Ullrich, A. (2000) *J. Bacteriol.* **182,** 5425–5432
22. Singh, R., Rao, V., Shakila, H., Gupta, R., Khera, A., Dhar, N., Singh, A., Koul, A., Singh, Y., Naseema, M., Narayanan, P. R., Paramasivan, C. N., Ramanathan, V. D., and Tyagi, A. K. (2003) *Mol. Microbiol.* **50,** 751–762
23. Cai, L., Holoweckyj, N., Schaller, M. D., and Bear, J. E. (2005) *J. Biol. Chem.* **280,** 31913–31923
24. Foger, N., Rangell, L., Danilenko, D. M., and Chan, A. C. (2006) *Science* **313,** 839–842